

## Dynamical spin susceptibility of ferromagnetic nickel

Ramjit Singh and Joginder Singh

*Physics Department, Panjab University, Chandigarh-160014, India*

Satya Prakash

*Laboratoire de Chimie Physique, Batiment 350, Avenue Jean Perrin 91405 Orsay, France*

(Received 21 September 1976)

The frequency- and wave-number-dependent spin susceptibility of ferromagnetic nickel is investigated using a noninteracting-spin band model constructed with the help of detailed band-structure calculations of Callaway and Wang. The free-electron approximation is used for electrons in the  $s$  band and the simple tight-binding wave function is used for electrons in the  $d$  subbands. The calculations for the diagonal part of susceptibility function are carried out for the field wave vector  $\vec{q}$  along the three principal symmetry directions [100], [110], and [111], and the anisotropy is found to be quite small. Therefore the only results along [100] direction are reported in this paper. The contribution of minority spin ( $\downarrow$ ) bands is found to be much larger than the contribution of majority spin ( $\uparrow$ ) bands. The total diagonal part of the susceptibility function is compared with the results for the paramagnetic phase. It is found that the susceptibility function of nickel in the ferromagnetic phase is larger than that in the paramagnetic phase.

### I. INTRODUCTION

The frequency- and wave-number-dependent susceptibility describes the response of a system to an applied field and is an important property in the study of many physical properties of the system. Considerable progress has been made in recent years in the understanding of ferromagnetic metals in terms of the itinerant model. Izuyama, Kim, and Kubo<sup>1</sup> have shown that spin waves which arise naturally from the Heisenberg model also may be obtained from this model. A more far reaching test of the itinerant model is the comparison of the predicted and measured differential cross section for the inelastic scattering of neutrons. This was done by Lowde and Windsor,<sup>2</sup> who in their comprehensive paper gave a very detailed analysis of their measurements on the magnetic response function of nickel. Their calculations were based upon a one-band model since interference between partial susceptibilities arising from the various bands were neglected. For the inelastic scattering cross section, Thompson<sup>3</sup> discussed scattering by Stoner single-particle modes at low temperatures for a short-range interaction single-band model of a ferromagnetic metal. Yamada and Shimizu<sup>4</sup> evaluated dynamical susceptibility of ferromagnetic nickel in a two-band model scheme. Kim *et al.*<sup>5</sup> discussed the spin and charge susceptibility of ferromagnetic electron gas including exchange interaction. Gillan<sup>6</sup> and Sokoloff<sup>7</sup> calculated the spin susceptibilities in the many-band and the one-band case, respectively, but both authors took a simplified view of the form

factors. All these authors have calculated susceptibilities treating electrons either in the free-electron approximation or in the tight-binding approximation. In transition metals the conduction electrons are neither totally free nor completely bound. An appropriate wave function for conduction electrons in these metals should include both the plane-wave and tight-binding parts. Hayashi and Shimizu<sup>8</sup> derived the generalized susceptibility for a single-band model of  $d$  electrons and for a two-band model of  $d$  and  $s$  electrons and applied it to calculate the impurity screening and induced spin density of ferromagnetic nickel using an effective-mass approximation for energy bands.

In the preceding paper,<sup>9</sup> hereafter referred to as I, we investigated the frequency- and wave-vector-dependent spin susceptibility of paramagnetic nickel for various values of momentum and energy transfer. A free-electron approximation for  $s$  electrons and the simple tight-binding wave function for  $d$  electrons was used while evaluating the various contributions to the susceptibility function. The scattering function calculated from the unenhanced and the exchange-enhanced reduced dynamical spin susceptibility fitted well with the earlier theoretical calculations and experimental measurements. In order to make a qualitative and quantitative comparison of dynamical spin susceptibility of nickel in the paramagnetic and ferromagnetic phase, we extend in this paper our calculations for the evaluation of the dynamical spin susceptibility of ferromagnetic nickel for the atomic configuration  $(3d)^{8,4}(4s)^{0,6}$ . We used the noninteracting spin band model due to Singh and

Prakash,<sup>10</sup> constructed with the help of the detailed band-structure calculations of Callaway and Wang.<sup>11</sup> The plan of the paper is as follows: the formalism is presented in Sec. II; the calculations and results are presented in Sec. III; and these are discussed in Sec. IV.

## II. THEORY

The generalized spin-dependent dynamical susceptibility obtained self-consistently in the Hartree approximation, ignoring local-field corrections, is

$$\chi^0(\vec{q}, \omega) = \mathcal{L}_{\epsilon \rightarrow 0} \frac{1}{4} g^2 \mu_B^2 \sum_{l'm'\sigma'} \sum_{\vec{k}, \vec{k}'} \frac{n_{l'm\sigma}(\vec{k}) - n_{l'm'\sigma'}(\vec{k}')}{E_{l'm'\sigma'}(\vec{k}') - E_{l'm\sigma}(\vec{k}) - \hbar\omega + i\epsilon} \langle \psi_{l'm\sigma}(\vec{k}) | e^{-i\vec{q}\cdot\vec{r}} | \psi_{l'm'\sigma'}(\vec{k}') \rangle \langle \psi_{l'm'\sigma'}(\vec{k}') | e^{i\vec{q}\cdot\vec{r}} | \psi_{l'm\sigma}(\vec{k}) \rangle. \quad (1)$$

Here  $n_{l'm\sigma}(\vec{k})$  is the Fermi occupation probability function which is unity for an occupied state and zero otherwise.  $\psi_{l'm\sigma}(\vec{k})$  and  $E_{l'm\sigma}(\vec{k})$  are the Bloch function and energy eigenvalue, respectively, for the electron with wave vector  $\vec{k}$ .  $l$ ,  $m$ , and  $\sigma$  are the orbital, magnetic, and spin quantum numbers, respectively, and act as band indices.  $\vec{q}$  is the field wave vector and  $\omega$  is the frequency of the applied magnetic field.  $\epsilon$  is a small positive infinitesimal corresponding to the adiabatic turning on of the perturbing field. The summation is over all the occupied electronic states.  $\vec{k}$  and  $\vec{k}' (= \vec{k} + \vec{q})$  are restricted in the first Brillouin zone.

Because of the orthogonality of the spin-wave functions, Eq. (1) simplifies to

$$\chi^0(\vec{q}, \omega) = [\chi_{\uparrow\uparrow}^0(\vec{q}, \omega) + \chi_{\downarrow\downarrow}^0(\vec{q}, \omega)], \quad (2)$$

where

$$\chi_{\sigma\sigma}^0(\vec{q}, \omega) = \mathcal{L}_{\epsilon \rightarrow 0} \frac{1}{4} g^2 \mu_B^2 \sum_{\vec{k}, \vec{k}'} \sum_{l'm\sigma} \frac{n_{l'm\sigma}(\vec{k}) - n_{l'm\sigma}(\vec{k}')}{E_{l'm\sigma}(\vec{k}') - E_{l'm\sigma}(\vec{k}) - \hbar\omega + i\epsilon} \times \langle \psi_{l'm\sigma}(\vec{k}) | e^{-i\vec{q}\cdot\vec{r}} | \psi_{l'm\sigma}(\vec{k}') \rangle \times \langle \psi_{l'm\sigma}(\vec{k}') | e^{i\vec{q}\cdot\vec{r}} | \psi_{l'm\sigma}(\vec{k}) \rangle. \quad (3)$$

$\chi_{\uparrow\uparrow}^0$  and  $\chi_{\downarrow\downarrow}^0$  are the charge susceptibility functions for the up- and down-spin electrons, respectively. Symbolically, in terms of the contributions to the susceptibility from various intraband and interband transitions, we can write  $\chi^0(\vec{q}, \omega)$  as

$$\chi^0(\vec{q}, \omega) = \sum_{\sigma} [\chi_{ss}^{\sigma}(\vec{q}, \omega) + \chi_{dd}^{\sigma}(\vec{q}, \omega) + \chi_{ds}^{\sigma}(\vec{q}, \omega) + \chi_{sd}^{\sigma}(\vec{q}, \omega)]. \quad (4)$$

Here  $\chi_{ss}^{\sigma}$ ,  $\chi_{dd}^{\sigma}$ ,  $\chi_{ds}^{\sigma}$ , and  $\chi_{sd}^{\sigma}$  are the contributions to the susceptibility function arising from the transitions from  $s$  band to  $s$  band,  $d$  subband to  $d$  subband,  $d$  subband to  $s$  band, and  $s$  band to  $d$  subband, respectively. The real and imaginary parts of the spin susceptibility are separated using the identity

$$\mathcal{L}_{\epsilon \rightarrow 0} \frac{1}{x \pm i\epsilon} = \frac{1}{x} \mp i\pi\delta(x) \quad (5)$$

and are evaluated in the same manner as described in I. The formalism for spin susceptibility extended to the ferromagnetic phase is given here in brief. Using the free-electron approximation for the wave function, and parabolic band approximation for the energies of electrons in the  $s$  band, we get the following familiar expressions for  $\text{Re}\chi_{ss}^{\sigma}(\vec{q}, \omega)$ , and  $\text{Im}\chi_{ss}^{\sigma}(\vec{q}, \omega)$ :

$$\text{Re}\chi_{ss}^{\sigma}(\vec{q}, \omega) = \frac{g^2 \mu_B^2}{8\pi^2} N\Omega_0 m_{s\sigma} k_{F s\sigma} \left\{ \frac{1}{2} + \frac{1}{8\lambda} \left[ 1 - \left( \frac{m_{s\sigma}\omega}{\lambda} - \lambda \right)^2 \right] \ln \left| \frac{1 - \frac{m_{s\sigma}\omega}{\lambda} + \lambda}{1 + \frac{m_{s\sigma}\omega}{\lambda} - \lambda} \right| - \frac{1}{8\lambda} \left[ 1 - \left( \frac{m_{s\sigma}\omega}{\lambda} + \lambda \right)^2 \right] \ln \left| \frac{1 - \frac{m_{s\sigma}\omega}{\lambda} - \lambda}{1 + \frac{m_{s\sigma}\omega}{\lambda} + \lambda} \right| \right\}, \quad (6)$$

$$\text{Im}\chi_{ss}^{\sigma}(\vec{q}, \omega) = -\frac{g^2 \mu_B^2}{64\pi\lambda} N\Omega_0 m_{s\sigma} k_{F s\sigma} \left\{ \left[ 1 - \left( \frac{m_{s\sigma}\omega}{\lambda} - \lambda \right)^2 \right] \theta \left[ 1 - \left( \frac{m_{s\sigma}\omega}{\lambda} - \lambda \right)^2 \right] - \left[ 1 - \left( \frac{m_{s\sigma}\omega}{\lambda} + \lambda \right)^2 \right] \theta \left[ 1 - \left( \frac{m_{s\sigma}\omega}{\lambda} + \lambda \right)^2 \right] \right\}, \quad (7)$$

where

$$\lambda = q/2k_{F_{s\sigma}}, \quad w = \omega/2k_{F_{s\sigma}}^2. \quad (8)$$

$\theta(x)$  is again a step function, which is unity if  $x \geq 0$  and zero otherwise.  $N$  is the number of unit cells in the crystal and  $\Omega_0$  is the volume of unit cell.  $m_{s\sigma}$  and  $k_{F_{s\sigma}}$  are the effective mass and Fermi momentum of  $s$  electrons of spin  $\sigma$ .

Using simple tight-binding wave functions and parabolic band approximations for electrons in the  $d$  subbands, the expressions for real and imaginary parts of  $\chi_{dd}^{\sigma}(\vec{q}, \omega)$  for the intraband transitions are obtained as follows:

$$\text{Re}\chi_{dd}^{\sigma}(\vec{q}, \omega) = \frac{g^2 \mu_B^2}{8\pi^2} N\Omega_0 \sum_m m_{dm\sigma} k_{F_{dm\sigma}} I_{dm} \left\{ \frac{1}{2} + \frac{1}{8\lambda'} \left[ 1 - \left( \frac{m_{dm\sigma} w'}{\lambda'} - \lambda' \right)^2 \right] \ln \left| \frac{1 - m_{dm\sigma} w'/\lambda' + \lambda'}{1 + m_{dm\sigma} w'/\lambda' - \lambda'} \right| \right. \\ \left. - \frac{1}{8\lambda'} \left[ 1 - \left( \frac{m_{dm\sigma} w'}{\lambda'} + \lambda' \right)^2 \right] \ln \left| \frac{1 - m_{dm\sigma} w'/\lambda' - \lambda'}{1 + m_{dm\sigma} w'/\lambda' + \lambda'} \right| \right\}, \quad (9)$$

$$\text{Im}\chi_{dd}^{\sigma}(\vec{q}, \omega) = -\frac{g^2 \mu_B^2 N\Omega_0}{64\pi\lambda'} \sum_m m_{dm\sigma} k_{F_{dm\sigma}} I_{dm} \left\{ \left[ 1 - \left( \frac{m_{dm\sigma} w'}{\lambda'} - \lambda' \right)^2 \right] \theta \left[ 1 - \left( \frac{m_{dm\sigma} w'}{\lambda'} - \lambda' \right)^2 \right] \right. \\ \left. \times \left[ 1 - \left( \frac{m_{dm\sigma} w'}{\lambda'} + \lambda' \right)^2 \right] \theta \left[ 1 - \left( \frac{m_{dm\sigma} w'}{\lambda'} + \lambda' \right)^2 \right] \right\}, \quad (10)$$

where

$$\lambda' = q/2k_{F_{dm\sigma}}, \quad w' = \omega/2k_{F_{dm\sigma}}^2, \quad (11)$$

and  $I_{dm}$  is the same as reported in I.  $m_{dm\sigma}$  and  $k_{F_{dm\sigma}}$  are the effective masses and Fermi momenta for the  $d$  electrons of spin  $\sigma$  in the  $m_{th}$   $d$  subband. Watson's<sup>12</sup> neutral atom  $3d$ -radial wave function is used in the present calculation, and therefore the matrix elements  $\langle \psi_{im\sigma}(\vec{k}) | e^{i\vec{q}\cdot\vec{r}} | \psi_{i'm'\sigma}(\vec{k} + \vec{q}) \rangle$  become the same for both up- and down-spin electrons, while the energy-dependent part of the susceptibility function remains spin dependent.

For the inter- $d$  subband transitions, i.e., when  $m \neq m'$ , the analytical expressions for the real and the imaginary parts of  $\chi_{dd}^{\sigma}(\vec{q}, \omega)$  are given as follows:

$$\chi_{dd}^{\sigma}(\vec{q}, \omega) = \sum_{m \neq m'} (I_1 + iI_2) \Delta_{dm, dm'}(\vec{q}) \Delta_{dm, dm'}^*(\vec{q}), \quad (12)$$

where

$$I_1 = -\frac{g^2 \mu_B^2 N\Omega_0}{8\pi^2} \left[ m_{dm'\sigma} \left( \frac{k_{F_{dm\sigma}}}{\xi} - X_1 - \frac{1}{4\xi^2} Y_1 \right) + m_{dm\sigma} \left( \frac{k_{F_{dm'\sigma}}}{\xi'} - X_2 - \frac{1}{4\xi'^2} Y_2 \right) \right] \quad (13)$$

$$X_1 = \left[ \frac{k_{F_{dm\sigma}}^2}{4q} - \frac{q}{4\xi} \left( 1 + \frac{2}{\xi} \right) + \frac{m_{dm'\sigma} \omega}{2\xi q} \right] \ln \left| \frac{2k_{F_{dm\sigma}} q - \xi k_{F_{dm\sigma}}^2 + q^2 - 2m_{dm'\sigma} \omega}{2k_{F_{dm\sigma}} q + \xi k_{F_{dm\sigma}}^2 - q^2 + 2m_{dm'\sigma} \omega} \right|, \quad (14)$$

$$X_2 = \left[ \frac{k_{F_{dm'\sigma}}^2}{4q} - \frac{q}{4\xi'} \left( 1 + \frac{2}{\xi'} \right) - \frac{m_{dm\sigma} \omega}{2\xi' q} \right] \ln \left| \frac{2k_{F_{dm'\sigma}} q - \xi k_{F_{dm'\sigma}}^2 + q^2 + 2m_{dm\sigma} \omega}{2k_{F_{dm'\sigma}} q + \xi k_{F_{dm'\sigma}}^2 - q^2 - 2m_{dm\sigma} \omega} \right|, \quad (15)$$

$$Y_1 = \Delta \begin{cases} \frac{2}{\sqrt{\Delta}} \left( \arctan \frac{2(\xi k_{F_{dm\sigma}} + q)}{\sqrt{\Delta}} + \arctan \frac{2(\xi k_{F_{dm\sigma}} - q)}{\sqrt{\Delta}} \right) & \text{if } \Delta > 0, \\ \frac{1}{\sqrt{-\Delta}} \left( \ln \left| \frac{2\xi k_{F_{dm\sigma}} + 2q - \sqrt{-\Delta}}{2\xi k_{F_{dm\sigma}} + 2q + \sqrt{-\Delta}} \right| + \ln \left| \frac{2\xi k_{F_{dm\sigma}} - 2q - \sqrt{-\Delta}}{2\xi k_{F_{dm\sigma}} - 2q + \sqrt{-\Delta}} \right| \right) & \text{if } \Delta < 0, \end{cases} \quad (16)$$

$$Y_2 = \Delta' \begin{cases} \frac{2}{\sqrt{\Delta'}} \left( \arctan \frac{2(\xi' k_{F_{dm'\sigma}} + q)}{\sqrt{\Delta'}} + \arctan \frac{2(\xi' k_{F_{dm'\sigma}} - q)}{\sqrt{\Delta'}} \right) & \text{if } \Delta' > 0, \\ \frac{1}{\sqrt{-\Delta'}} \left( \ln \left| \frac{2\xi' k_{F_{dm'\sigma}} + 2q - \sqrt{-\Delta'}}{2\xi' k_{F_{dm'\sigma}} + 2q + \sqrt{-\Delta'}} \right| + \ln \left| \frac{2\xi' k_{F_{dm'\sigma}} - 2q - \sqrt{-\Delta'}}{2\xi' k_{F_{dm'\sigma}} - 2q + \sqrt{-\Delta'}} \right| \right) & \text{if } \Delta' < 0, \end{cases} \quad (17)$$

$$\Delta = -4[q^2(\xi + 1) - 2m_{dm'\sigma} \omega \xi], \quad \xi = m_{dm'\sigma}/m_{dm\sigma} - 1, \quad (18)$$

$$\Delta' = -4[q^2(\xi' + 1) + 2m_{dm\sigma} \omega \xi'], \quad \xi' = m_{dm\sigma}/m_{dm'\sigma} - 1, \quad (19)$$

$$I_2 = -(g^2 \mu_B^2 N \Omega_0 / 32 \pi q) (Z_1 + Z_2), \quad (20)$$

where

$$Z_1 = m_{dm'\sigma} \begin{cases} k_{Fdm\sigma}^2 - k_1^2 & \text{if } k_1 < k_{Fdm\sigma} < k_2, \quad \mu_1 \geq 0 \\ k_2^2 - k_1^2 & \text{if } k_2 < k_{Fdm\sigma}, \quad \mu_1 \geq 0 \\ 0 & \text{if } k_{Fdm\sigma} < k_1, \quad \mu_1 \geq 0 \\ 0 & \text{if } \mu_1 < 0, \end{cases} \quad (21)$$

$$Z_2 = m_{dm\sigma} \begin{cases} k_{Fdm'\sigma}^2 - k_1'^2 & \text{if } k_1' < k_{Fdm'\sigma} < k_2', \quad \mu_2 \geq 0 \\ k_2'^2 - k_1'^2 & \text{if } k_2' < k_{Fdm'\sigma}, \quad \mu_2 \geq 0 \\ 0 & \text{if } k_{Fdm'\sigma} < k_1', \quad \mu_2 \geq 0 \\ 0 & \text{if } \mu_2 < 0, \end{cases} \quad (22)$$

$$\mu_1 = -\Delta / 4m_{dm'\sigma}^2, \quad (23)$$

$$\mu_2 = -\Delta' / 4m_{dm\sigma}^2. \quad (24)$$

$k_1, k_2, k_1', k_2'$  are the same as reported in I.

Using the free-electron approximation for  $s$  electrons and the simple tight-binding wave function for  $d$  electrons, the tractable expressions for the real and imaginary parts of  $\chi_{ds}^\sigma(\vec{q}, \omega)$  and  $\chi_{sd}^\sigma(\vec{q}, \omega)$  are obtained as follows:

$$\begin{aligned} \text{Re} \chi_{ds}^\sigma(\vec{q}, \omega) = & \frac{g^2 \mu_B^2 N m_{s\sigma} (48)^2}{\pi} \sum_i \sum_j a_i a_j \alpha_i \alpha_j \sum_m (-1)^m \int_0^{k_{Fdm\sigma}} \frac{dk k^6}{(k^2 + \alpha_i^2)^4 (k^2 + \alpha_j^2)^4} \\ & \times [D_{0m}^2 D_{0-m}^2 I_0^1 + (D_{1m}^2 D_{-1-m}^2 + D_{-1m}^2 D_{1-m}^2) I_1^1 \\ & + (D_{2m}^2 D_{-2-m}^2 + D_{-2m}^2 D_{2-m}^2) I_2^1], \end{aligned} \quad (25)$$

$$\begin{aligned} \text{Im} \chi_{ds}^\sigma(\vec{q}, \omega) = & -g^2 \mu_B^2 N m_{s\sigma} (48)^2 \sum_i \sum_j a_i a_j \alpha_i \alpha_j \sum_m (-1)^m \int_0^{k_{Fdm\sigma}} \frac{dk k^6}{(k^2 + \alpha_i^2)^4 (k^2 + \alpha_j^2)^4} \\ & \times [D_{0m}^2 D_{0-m}^2 I_0^2 + (D_{1m}^2 D_{-1-m}^2 + D_{-1m}^2 D_{1-m}^2) I_1^2 \\ & + (D_{2m}^2 D_{-2-m}^2 + D_{-2m}^2 D_{2-m}^2) I_2^2], \end{aligned} \quad (26)$$

$$\begin{aligned} \text{Re} \chi_{sd}^\sigma(\vec{q}, \omega) = & \frac{g^2 \mu_B^2 N (48)^2}{\pi} \sum_i \sum_j a_i a_j \alpha_i \alpha_j \sum_m (-1)^m m_{dm\sigma} \int_0^{k_{Fds\sigma}} dk k^2 [D_{0m}^2 D_{0-m}^2 I_0^3 + (D_{1m}^2 D_{-1-m}^2 + D_{-1m}^2 D_{1-m}^2) I_1^3 \\ & + (D_{2m}^2 D_{-2-m}^2 + D_{-2m}^2 D_{2-m}^2) I_2^3], \end{aligned} \quad (27)$$

$$\begin{aligned} \text{Im} \chi_{sd}^\sigma(\vec{q}, \omega) = & -g^2 \mu_B^2 N (48)^2 \sum_i \sum_j a_i a_j \alpha_i \alpha_j \sum_m (-1)^m m_{dm\sigma} \int_0^{k_{Fds\sigma}} dk k^2 [D_{0m}^2 D_{0-m}^2 I_0^4 + (D_{1m}^2 D_{-1-m}^2 + D_{-1m}^2 D_{1-m}^2) I_1^4 \\ & + (D_{2m}^2 D_{-2-m}^2 + D_{-2m}^2 D_{2-m}^2) I_2^4], \end{aligned} \quad (28)$$

where  $I_0^1, I_1^1, I_2^1, I_0^2, I_1^2, I_2^2, I_0^3, I_1^3, I_2^3, I_0^4, I_1^4, I_2^4$  are the same as reported in I. The rotation matrices  $D_{mm'}$  with argument  $(-\gamma, -\beta, -\alpha)$  (Euler angles) are taken from Prakash and Joshi.<sup>13</sup> The radial integrations are carried out numerically.

### III. CALCULATIONS AND RESULTS

#### A. Model band structure

The energy-band calculations for ferromagnetic nickel have been done by several authors. We use

the noninteracting spin band model of Singh and Prakash<sup>10</sup> constructed with the help of more recent band-structure calculations of Callaway and Wang.<sup>11</sup> The Fermi momenta and effective masses are taken from the paper by Singh and Prakash.<sup>10</sup> All the majority spin  $d$  subbands are completely filled, but the  $s$  band is partially filled. Two minority spin  $d$  subbands and  $s$  bands are partially filled. In response to the applied magnetic field the electrons redistribute their energies and undergo the following transitions: (i) intraband transi-

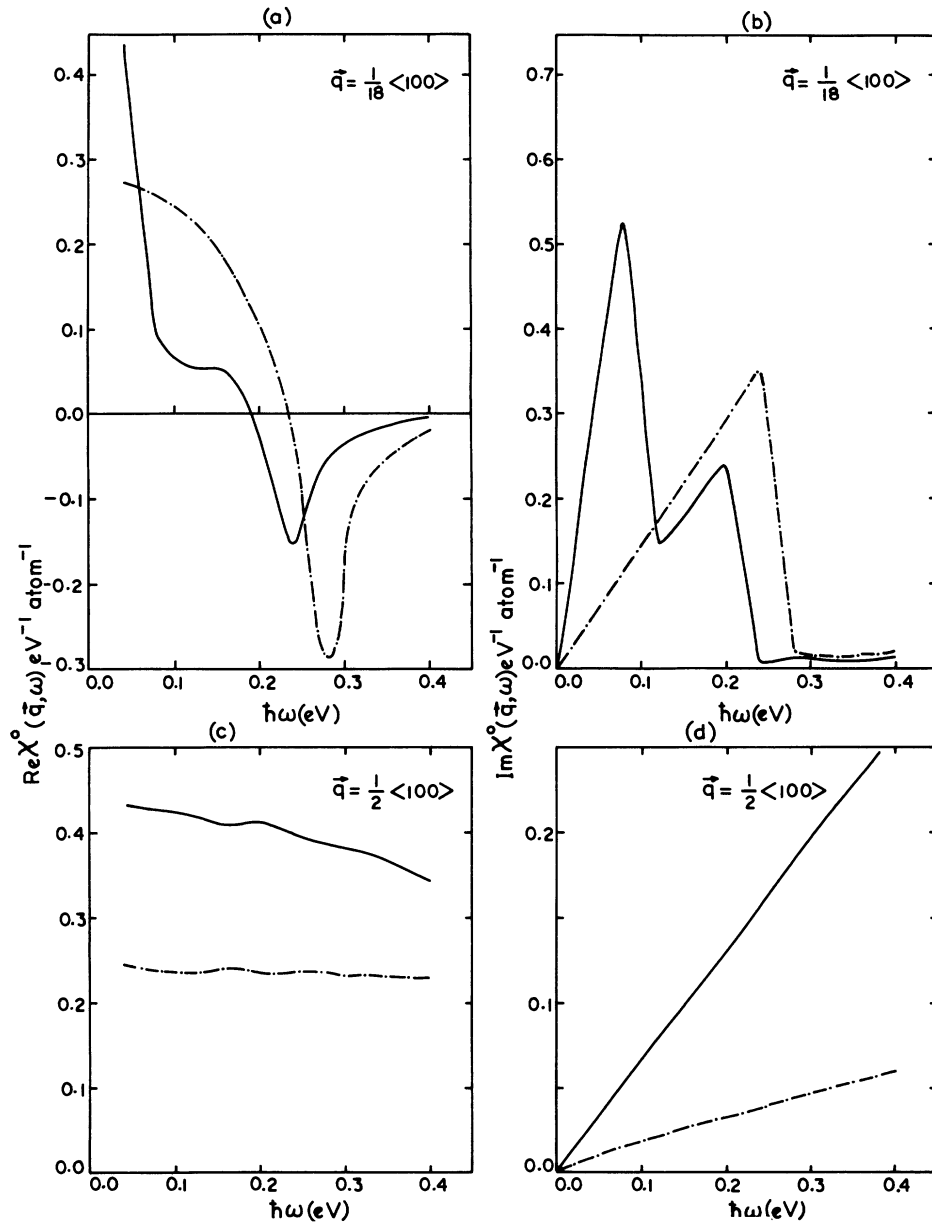


FIG. 1.  $X^0(\vec{q}, \omega)$  vs  $\hbar\omega$  for nickel. The solid lines represent the susceptibility function for ferromagnetic nickel and the dash-dot lines represent susceptibility for paramagnetic nickel.  $X^0(\vec{q}, \omega)$  is measured in units of  $g^2\mu_B^2$ .

tions in partially filled majority and minority spin  $s$  bands; (ii) interband transitions from filled majority spin  $d$  subbands to partially filled majority spin  $s$  bands; (iii) intraband transitions in partially filled minority spin  $d$  subbands and interband transitions from partially and completely filled minority spin  $d$  subbands to partially filled minority spin  $s$  and  $d$  subbands; (iv) interband transitions from partially filled minority spin  $s$  bands to partially filled minority spin  $d$  subbands. The hybridization between different  $m$  components of the  $d$  wave function has been taken into account by giving equal weight to all the  $m$  values of each  $d$  subband.

#### B. Unenhanced susceptibility function

We first calculated the susceptibility along the three principal symmetry directions [100], [110], and [111]. Anisotropy was found to be small except in the vicinity of  $\vec{q}=0$ . In order to make qualitative and quantitative comparison of the susceptibility function of nickel in the paramagnetic and ferromagnetic phases we fixed  $\vec{q}$  along the [100] direction and evaluated the real and imaginary parts of the susceptibility function for ferromagnetic nickel for the atomic configuration  $(3d)^{9.4}(4s)^{0.6}$ . The results were obtained both by varying  $\vec{q}$  for fixed

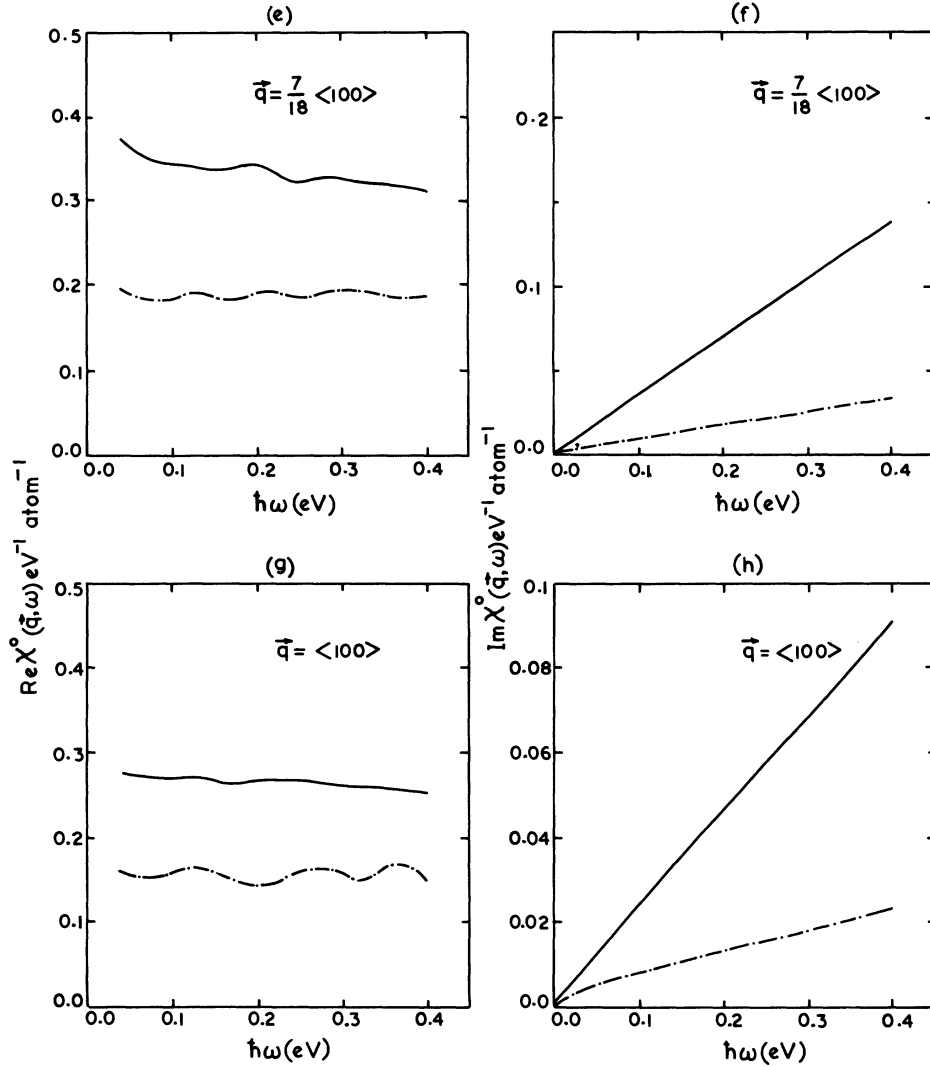


Fig. 1. (continued).

energy transfer and by varying  $\omega$  for fixed momentum transfer. The susceptibility variation with  $\omega$  is shown in Fig. 1, and with  $\vec{q}$  in Fig. 2. The results for paramagnetic Ni reported in I are also plotted in the same figures for comparison sake.

The contributions of  $\chi_{ss}^\dagger$  and  $\chi_{ss}^\downarrow$  are found to be almost equal because the majority and minority spin  $s$  bands almost overlap. The contribution  $\sum_{\sigma} \chi_{sd}^{\sigma}$  is only due to minority spin bands.  $\sum_{\sigma} \chi_{dd}^{\sigma}$  is 10–20 times larger than  $\sum_{\sigma} \chi_{ss}^{\sigma}$ . The major contribution to the dynamical susceptibility function comes from the minority spin bands because of partially filled  $d$  subbands and the dominating part in it is the intraband contribution ( $\chi_{ss}^\dagger + \chi_{dd}^\dagger$  for  $m = m'$ ). The total interband part

$$\sum_{\sigma} (\chi_{dd}^{\sigma} \text{ for } m \neq m' + \chi_{ds}^{\sigma} + \chi_{sd}^{\sigma})$$

is very small compared with the intraband part and

only adds to the oscillatory nature of total susceptibility function. The interband contribution increases with increasing  $\vec{q}$ , demonstrated by the pronounced oscillatory behavior of  $\text{Re}\chi^0(\vec{q}, \omega)$  at large  $\vec{q}$ , whereas the intraband contribution decreases smoothly with increasing  $\vec{q}$ . The trend of the real susceptibility is to decrease with both increasing  $\vec{q}$  and  $\omega$  but the decrement with  $\vec{q}$  is much larger in comparison with the decrement with  $\omega$ . The imaginary part of  $\chi^0(\vec{q}, \omega)$  increases with increasing  $\omega$  but decreases with increasing  $\vec{q}$ .

While intercomparing the spin susceptibility functions of nickel in the paramagnetic phase and ferromagnetic phase, we find that the magnitudes of both the real and imaginary parts of susceptibility in the ferromagnetic case are (30–80)% larger than that in paramagnetic case (which is to be expected). The susceptibility in low- $\vec{q}$  regions for the ferromagnetic phase is much larger than

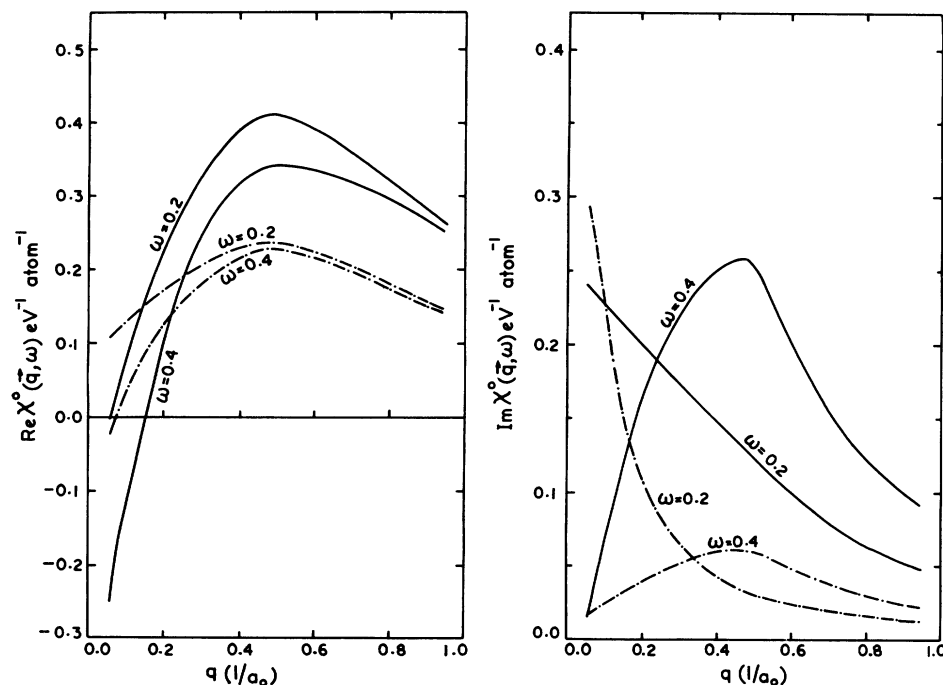


FIG. 2.  $X^0(\vec{q}, \omega)$  vs  $\vec{q}$  along the [100] direction. The solid lines represent the susceptibility for ferromagnetic nickel and the dash-dot lines represent the susceptibility for paramagnetic nickel.  $X^0(\vec{q}, \omega)$  is measured in units of  $g^2 \mu_B^2$ .  $q$  is measured in inverse Bohr units and  $\omega$  is in a.u.

that for the paramagnetic phase. The anomalous behavior of susceptibility at small values of  $\vec{q}$  is also found in ferromagnetic nickel, but the changes are more rapid and the peaks are shifted to lower values of  $\omega$ . The broad maxima at small values of  $\vec{q}$  for fixed energy transfers are also found in  $\text{Re} X^0(\vec{q}, \omega)$  of ferromagnetic nickel. The appearance of broad maxima is the consequence of inclusion of  $d$  bands in our calculations. The general qualitative behavior of real and imaginary susceptibility with the variation of  $\vec{q}$  as well as  $\omega$  for both the phases is nearly the same.

#### IV. DISCUSSION

In principle one must consider the interference between partial susceptibilities arising from the various bands which was neglected in our calculations. This contribution is, however, small since our calculations are confined to the first Brillouin zone only for the diagonal case.<sup>14</sup> The exchange and correlation corrections in the susceptibility function for the ferromagnetic phase are very important. The exact form of the exchange and

correlation corrections for  $d$  electrons is not well established and the inclusion of exchange and correlation corrections for  $s$  electrons will have little effect because  $\chi_{dd}^0$  is dominating. The resistivity of nickel calculated from exchange enhanced imaginary susceptibility will be presented in our following paper. One should use a wave function for  $s$  electrons which is orthogonal to core and  $d$  wave functions. An orthogonalized plane wave is a suitable choice but it has been found that orthogonalization corrections are very small,<sup>15</sup> and therefore the use of a simple plane wave for  $s$  electrons is fairly justified. The spin-orbit interaction has been neglected in our calculation since, as was pointed out, it is small in the case of nickel.<sup>16</sup>

#### ACKNOWLEDGMENTS

We express our thanks to Professor S. K. Joshi and Dr. K. N. Pathak for helpful discussions and Professor H. S. Hans for providing the necessary facilities in the department. The financial assistance from the Council of Scientific and Industrial Research, New Delhi (India) is also acknowledged.

<sup>1</sup>T. Izuyama, D. J. Kim and R. Kubo, J. Phys. Soc. Jpn. 18, 1025 (1963).

<sup>2</sup>R. D. Lowde and C. G. Windsor, Adv. Phys. 19, 813 (1970).

<sup>3</sup>E. D. Thompson, Phys. Rev. Lett. 19, 635 (1967).

<sup>4</sup>H. Yamada and M. Shimizu, J. Phys. Soc. Jpn. 22, 1404 (1967).

<sup>5</sup>D. J. Kim, B. B. Schwartz, and H. C. Pradhaude, Phys. Rev. B 7, 205 (1973).

<sup>6</sup>M. J. Gillan, J. Phys. F 3, 1874 (1973).

- <sup>7</sup>J. B. Sokoloff, Phys. Rev. 180, 613 (1969); 185, 770 (1969); 185, 783 (1969).
- <sup>8</sup>E. Hyashi and M. Shimizu, J. Phys. Soc. Jpn. 26, 1396 (1969); 27, 43 (1969).
- <sup>9</sup>Ramjit Singh and Satya Prakash, Phys. Rev. B (to be published).
- <sup>10</sup>Natthi Singh, Joginder Singh, and Satya Prakash, Phys. Rev. B 12, 1076 (1975).
- <sup>11</sup>J. Callaway and C. S. Wang, Phys. Rev. B 7, 1096 (1973).
- <sup>12</sup>R. E. Watson, MIT Solid State and Molecular Theory Group Technical Report No. 12 (1952) (unpublished).
- <sup>13</sup>S. Prakash and S. K. Joshi, Phys. Rev. B 2, 915 (1970).
- <sup>14</sup>D. G. Clark and W. Young, J. Phys. C 7, 3103 (1974).
- <sup>15</sup>W. R. Hanke, Phys. Rev. B 8, 4558 (1973).
- <sup>16</sup>Nobuo Mori, J. Phys. Soc. Jpn. 25, 72 (1968); 25, 1249 (1968).